Detection of Dementia Through 3D Convolutional Neural Networks Based on Amyloid PET

Giovanna Castellano
Department of Computer Science
University of Bari Aldo Moro
Bari, Italy
0000-0002-6489-8628

Andrea Esposito
Department of Computer Science
University of Bari Aldo Moro
Bari, Italy
0000-0002-9536-3087

Marco Mirizio
Department of Computer Science
University of Bari Aldo Moro
Bari, Italy

Graziano Montanaro
Department of Computer Science
University of Bari Aldo Moro
Bari, Italy

Gennaro Vessio
Department of Computer Science
University of Bari Aldo Moro
Bari, Italy
0000-0002-0883-2691

***Abstract*—Dementia is one of the most common diseases in the elderly and a leading cause of mortality and disability. In recent years, a research effort has been made to develop computer aided diagnosis tools based on machine (deep) learning models fed with neuroimaging data. However, while much work has been done on MRI imaging, very little attention has been paid on amyloid PETs, which have been recently recognized to be a promising and powerful biomarker of neurodegeneration. In this paper, we contribute to this less explored research area by proposing a 3D Convolutional Neural Network aimed at detecting dementia based on amyloid PET scans. An experiment performed on the recently released OASIS-3 dataset, which provides the community with a new benchmark to advance this line of research further, yielded very promising results and provided new evidence on the effectiveness of amyloid PET.**

***Index Terms*—dementia, Alzheimer's, amyloid PET, computer aided diagnosis, deep learning, convolutional neural networks**

I. Introduction

Dementia is one of the most common diseases in the elderly and a leading cause of mortality and disability [1]: neurodegenerative disorders affect about 15% of the entire world population and, in the US alone, more than 5 million of individuals are suffering from some kind of cognitive disorder, of which about 60% are results of Alzheimer's disease (AD) [2]. Dementia, in fact, is not a syndrome but rather a symptom of an underlying disease that depends on the patient's age [3]. For example, in younger patients, Huntington's disease and genetic forms of AD tend to occur more often; while, in older patients, cognitive problems are often due to AD, Lewy body dementia, and vascular diseases [3], [4].

2021 IEEE Symposium Series on Computational Intelligence (SSCI)
DOI: 10.1109/SSCI50451.2021.9660102

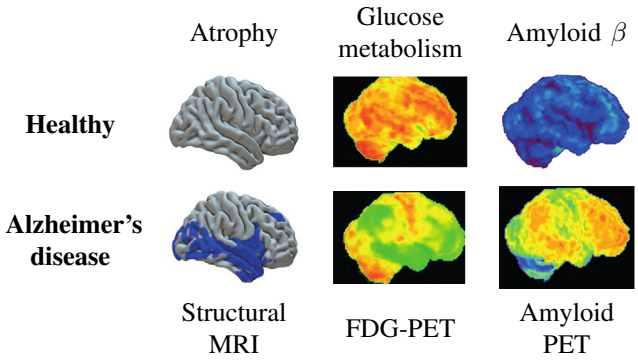

Fig. 1: Neuroimaging obtained with structural MRI or PET using different radiotracers both in healthy subjects and in subjects with AD (adapted from [7]).

An accurate and early diagnosis of dementia makes it possible to implement an intervention to slow down the progression of the disease. Unfortunately, the time between the onset of symptoms and diagnosis is often long [5], due to the insidious onset of the disease and the lack of recognition by families or the uncertainty of the diagnostic path [6]. Various attempts have been made in the medical field to diagnose neurodegenerative diseases, and more specifically dementia, as early as possible, and Artificial Intelligence aims to help clinicians recognize underlying diseases that impair patients' cognitive abilities.

Among the attempts to diagnose dementia in the pre-clinical stage, several works, e.g. [8]–[13], have proposed diagnostic models based on the analysis of MRI scans of the brain. Although the use of MRI scans is effective in finding scar tissue, necrosis, and/or atrophy in the brain, recent research has shown a high correlation between the amount of amyloid in the cerebral cortex and AD [7]. For this purpose, amyloid PET imaging represents a powerful biomarker for the assessment

of people with cognitive impairment [14]. The scan displays plaques in the brain, which are the main suspects of damaging and killing nerve cells in AD. Before amyloid PET, these plaques could only be detected by examining the brain during an autopsy.

In the medical field, PET scans are classified using the contrast material. The three PET scans widely used in the diagnosis and recognition of AD are PiB-PET, AV45-PET, and FDG-PET [14]. The main difference between each of the three types of PET scans lies in the substance used as the contrast material: PiB-PET scans use the Pittsburgh compound B (PiB), which binds to amyloid and tends to concentrate near the cerebral cortex of people with AD [15]; AV45-PET scans use florbetapir (AV45) which, like PIB, binds to amyloid [16]; finally, FDG-PET scans use fluorodeoxyglucose which, unlike the previous compounds, is used to evaluate glucose metabolism [17]. We can therefore group the available types of PET scans into two categories: amyloid PETs can be used to detect the concentration of amyloid in the brain; glucose PETs can be used to analyze glucose metabolism. Both types can be used as evidence in the diagnosis of AD [14] (as shown in Figure 1), but amyloid PETs are slightly more sensitive when used to diagnose AD, especially in patients with known histopathology [18]. Thus, we focus on amyloid PETs.

To the best of our knowledge, very few attempts have been made to create an automatic diagnostic tool for dementia and, more specifically, for AD using amyloid concentration (e.g., [19]). Even fewer works are based on the analysis of PET images, both for the evaluation of glucose metabolism and for the amount of amyloid. This paper aims to contribute to this research direction by proposing a model, based on a 3D Convolutional Neural Network (CNN), which allows the detection of dementia by amyloid PET scans. The method was tested on the recently proposed OASIS-3 dataset [20], which provided the community with a new benchmark for further advancing neurodegenerative disease research.

The rest of this paper is organized as follows. Section II discusses related works. Section III presents the dataset used to train and test the model built using the method discussed in Section IV. Section V details the experimental session and its results. Section VI provides conclusions and highlights possible improvements for future work.

II. Related Work

Although dementia is one of the most common neurodegenarative diseases, a preemptive diagnosis is still difficult. Indeed, dementia is considered highly under-diagnosed worldwide, and a correct diagnosis, if ever made, is usually in the advanced stage of the disease [21]. To help doctors in this difficult task, Artificial Intelligence can play an important role. Computational and AI-based solutions, in fact, have been used with promising results to support the analysis of similar or related disorders, e.g. [22]–[25].

Various attempts have been made to develop intelligent models that automatically analyze neuroimaging data, such as MRI and PET, to support the diagnosis of dementia. Structural MRI remains the standard neuroimaging technique and is used as a means to differentiate between AD and other types of dementia, as it helps estimate tissue damage or loss in vulnerable brain regions [26]. More precisely, MRI scans allow the quantification of the amount of atrophy in the brain, which is a valid marker and an inevitable step in neurodegenerative diseases. To this end, the work recently presented by Altay et al. [8] involves the use of neural networks to predict the incidence of AD using MRI scans. It is based on the same OASIS-3 dataset that we used in our study. As MRI images are 3D scans (created by taking multiple shots, or "slices", moving the scanner along an axis for a very short distance), one problem lies in processing the third dimension. A first approach consists in treating the volumes as a stream of 2D images, as happens in one of the models presented in [8]. Another approach is to modify the neural network to accept a 3D volume as its input, as suggested in [27]. Similar reasoning can also be applied to PET scans, as we did for our model.

While structural MRI is undoubtedly powerful, recent literature is also investigating on the contribution of amyloid PET to aid in the diagnosis of dementia. It can provide a complementary contribution, as it can allow the model to observe different features of the brain. In fact, it is now widely known that AD is closely related to the presence of β-amyloid (a peptide whose function is still unknown [28]) in the cerebral cortex [7]. Using PET scans, we can detect and quantify the concentration of this peptide (as well as many other substances) using a contrast material.

Most of the research work that aims to automatically recognize AD using PET scans uses FDG-PET scans. For example, the work presented by Ding et al. [29] uses a CNN trained on the ADNI dataset to diagnose Alzheimer's before the onset of symptoms. Few works attempt to use amyloid PET scans to achieve similar goals, although such scans are more sensitive in some cases (for example, if patients have known histopathology) [18]. A slightly larger number of researchers attempted to create a model that performs the diagnosis through both FDG and amyloid PETs, e.g. [19]. A limitation of this approach lies in the nature of the PET scans themselves: by grouping both FDG and amyloid scans as inputs for a single model, we can introduce biases due to the different underlying subject (glucose metabolism for FDG scans, β-amyloid for the others). A better approach may be to train different models: one for each type of PET scan. As this is a less explored area of research, this paper focuses on using amyloid PET scans as an input to a 3D convolutional neural network.

III. Materials

For the purposes of this study, we considered the OASIS-3 dataset [20], that is the latest version of the OASIS dataset already used by various authors for several research objectives [30]–[34]. It is a collection of MRI and PET images for 1098 participants, including 605 cognitively normal adults and 493 individuals in various stages of cognitive decline, aged 42 to 95. In this paper we focus on PET images. In particular, the

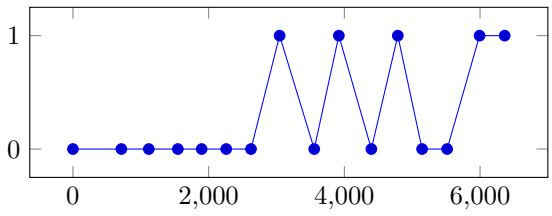

(a) Before

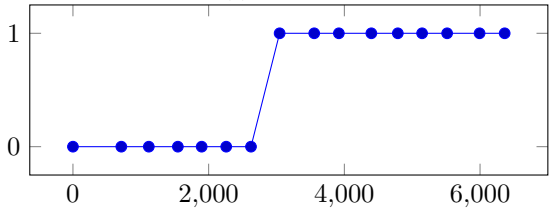

(b) After

Fig. 2: An example of the distribution of the labels before and after the post-processing step aimed at removing false positives and false negatives. In particular, the data of the subject "OAS30040" have been considered here. The horizontal axis indicates the days since entry.

dataset consists of 1607 PET sessions, which can be used to diagnose AD. Among these sessions, we considered the 1352 PET sessions, available as part of the dataset, which have already been post-processed using the PET Unified Pipeline - PUP. The OASIS-3 dataset provides the three different types of PET scans described in Section I, with different availability for each session, namely PiB-PET, AV45-PET, and FDG-PET. For the purpose of our work, we used only the amyloid PET scans (i.e., PiB-PET and AV45-PET), which comprise approximately 93% of the PET scan subset of the entire dataset. From an initial analysis of the available processed PET scans, multiple images are provided for each scanning session (such as the PET itself and an associated T1-weighted MRI): only PET scans were considered; more precisely, only those normalized with motion correction.

Given the complexity of the dataset, which includes diverse data and metadata associated with patients who have undergone more than one medical evaluation, pre-processing was required to make the data more suitable for neural network learning. First of all, since the OASIS-3 dataset does not provide directly pre-labeled images, a labeling step was required to provide the ground truth of the diagnostic model. The OASIS-3 dataset provides a list of psychiatric and neurological assessments for each patient, along with an evaluation of the cognitive state, using the Clinical Dementia Rating scale [35], and a possible diagnosis. Each entry is labeled by up to five different differential diagnoses expressed in natural language. First, all labels were mapped to a value of 0 (representing cases of "healthy" or "non-dementia diagnosis") or a value of 1 (representing the "AD or similar dementia diagnosis" cases), thus transforming the problem into a binary classification. Then, after this first step, all five differential diagnoses were merged into a single label, so that the final value is 1 if and only if at least one differential diagnosis falls into the "AD or similar dementia diagnosis" class. To further improve this step, each label was post-processed to remove as many false negatives and false positives as possible from the dataset. If the label was negative and at least one of the two predecessors was positive and at least one of the two successors was positive, then the label became positive; otherwise, if the label was positive and the immediate predecessor was not positive and the two successors were both negative, then the label became negative. The plot in Figure 2 represents the result of this post-processing phase. Finally, each PET scan image was assigned a label based on the latest diagnosis. Since not all scan sessions are associated with a psychiatric or neurological test, each scan was associated with the closest test in time (either way: before or after the scan).

After the first pre-processing step, a labeled dataset of PET scans was obtained. It consists of 1217 negative samples and only 135 positive samples. It is clear that, since $\sim 90\%$ of the samples are negative, this is a highly imbalanced dataset. To address this issue, we opted for a combination of random under-sampling of the negative class and the application of data augmentation techniques to the positive class. To perform the random under-sampling of the negative class, we first selected all negative scans of the same subjects that have positive scans: this would allow comparison between two images without any severe morphological difference in the brains represented. This selection yielded a total of 23 images. Then, we randomly selected a total of 182 scans from the remaining negative scans, reaching a total of 205 negative samples. Finally, we augmented the positive samples by about 50% (thus obtaining a total of 205 images) through random rotation and mirroring of some images (as recently performed by [8] on the same dataset).

IV. Methods

Most of the work in the literature that uses neural networks to detect dementia in neuroimaging data makes use of traditional feed-forward neural networks fed with flattened feature vectors, e.g. [36], or 2D convolutional neural networks that accept only single slices as inputs, e.g. [10], [29]. These approaches lead to ignoring the information that 3D volumes intrinsically carry on. To overcome this issue, in this study we propose to use a 3D convolutional neural network (3D CNN) taking the 3D volume as input.

Figure 3 shows the architecture of the proposed model. It is a 17-layer 3D CNN comprising four 3D convolutional layers with two layers consisting of 64 filters followed by 128 and 256 filters, all with a kernel size of $3 \times 3 \times 3$, as done in [37]. Each convolutional layer is followed by a max pooling layer with a stride of 2, again followed by a batch normalization layer. The sequence of the four groups of layers defines the feature extraction block of the model, which is followed by a dense layer of 512 neurons, which receives the flattened output of the feature extraction block, followed by a dropout

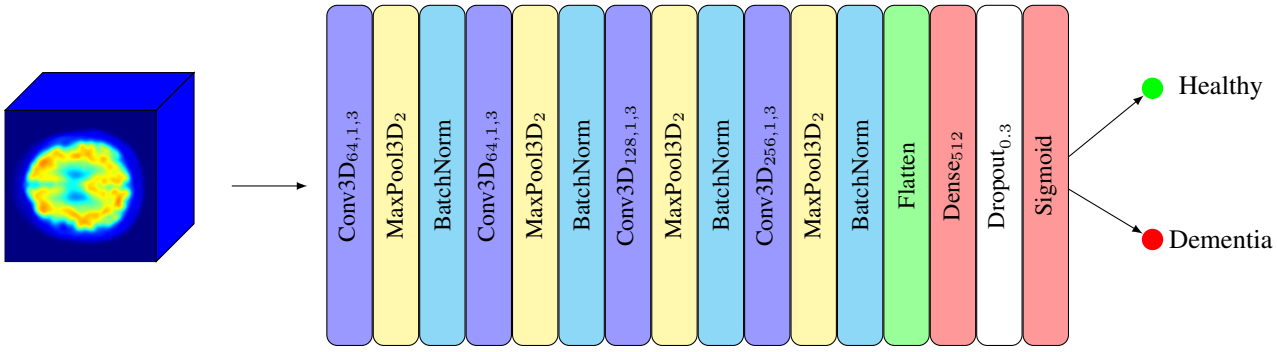

Fig. 3: The 3D CNN model. Subscripts indicate hyperparameters (# filters, stride and kernel size in the case of conv layers).

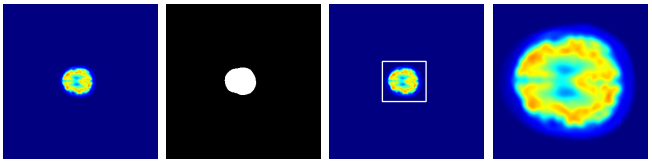

(a) Original scan (b) Thresholded (c) Bounding box (d) Final scan

Fig. 4: An example of the scaling and cropping process using the Otsu threshold.

layer (with a 30% dropout rate) and a sigmoid output neuron performing the binary classification.

Before training the model, another pre-processing step was required to resize the images. PET scans are 3D images (i.e., sequences of images depicting a different slice of the brain along an axis) taken during a predefined time interval. For this reason, the first step was to decide how to treat the time coordinate in the images. We chose to reduce the series of images over time to a single average image, thus allowing us to treat PET images as a typical MRI or CT image. Each averaged PET scan, therefore, required to be resized to a common size. To avoid introducing up-scaling artifacts, the image slices were resized to 128×128 voxels, the minimum size available in the dataset. A similar criterion was applied to the choice of the number of slices to keep for each image: to account for the diversity of the scan settings and, therefore, the diversity in the availability of the slices, we chose to keep the 50 middle slices as it is certain that they depict the subject's brain (similar to the choice of middle slices in [8]). Before scaling, the images were processed to identify a bounding box around the brain, in order to center it: first, a heavily blurred version (using a Gaussian blur with kernel size 13×13 and $\sigma = 150$) of the images were segmented using the simple, but effective Otsu thresholding [38]; then, a simple bounding box was selected by detecting the "high" values in the images (Fig. 4).

V. Experimental Results

The experiment was performed on Google Colaboratory Pro, using the GPU NVIDIA Tesla P100. The model architecture was implemented using the popular TensorFlow library.

To evaluate the proposed method, a *stratified* 10-fold cross-validation was used. In other words, each fold contained roughly the same proportions as the two types of class labels. For the training phase, we used binary cross-entropy as a loss function, defined as follows:

$$\mathcal{H}(y, p) = -\left(y \log(p) + (1 - y) \log(1 - p)\right),$$

where y is the ground truth label, while p is the model output for an individual observation. Cross-entropy was minimized using the Adam optimizer with a dynamic learning rate, with an exponential decay (rate 0.96) and a starting value of 5×10^{-5}. The maximum number of epochs was 10^4, with an early stopping criterion.

As performance metrics, we computed the following classic metrics commonly used in the diagnostic field:

- Accuracy: that is simply the proportion of correctly predicted samples (both true positives and true negatives) in the selected population;
- Sensitivity: which refers to the proportion of diseased subjects who have been classified as having the condition;
- Specificity: that is the proportion of healthy samples who have been classified as not affected by the disease;
- AUC (Area Under the ROC Curve): which is used as a summary of the ROC curve; the higher the AUC, the better the model performance in distinguishing between the positive and negative class.

Figure 5 shows the results of the stratified 10-fold cross-validation. It can be seen that the model achieved a relatively high and stable average accuracy of 83%, indicating the effectiveness of the proposed approach as a decision support tool. As for the other performance metrics, the model also showed a sensitivity and specificity of 86% and an AUC of 87%. This indicates that the model did not favor the classification of one class over the other and this may be due to the attention paid to balancing the dataset.

The results obtained are in line with several recently published results achieved on OASIS as well as ADNI with deep learning [39]. A schematic comparison with some of the more recent works is provided in Table I. Even though our results are not outstanding, they are quite promising considering that the task is very challenging and the community is still working

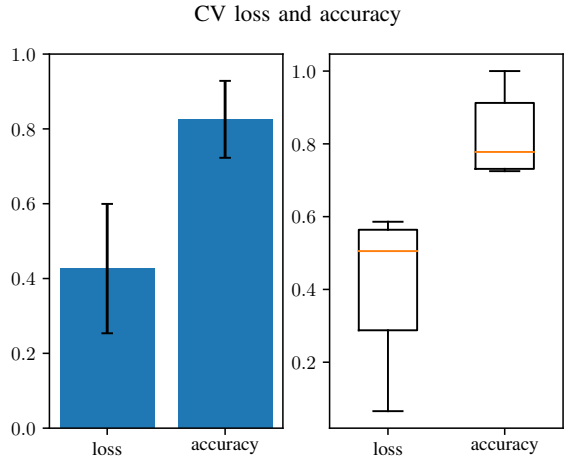

Fig. 5: Cross-validation results. The graph on the left represents the average accuracy and loss and their standard deviation; the graph on the right represents a box plot of all the losses and accuracies reached during the cross-validation.

to achieve generalizable results that drive this technology to finally reach technology transfer.

VI. Conclusion and Future Work

In this paper, we investigated whether amyloid PET scans could be a valuable diagnostic input to aid in the recognition and diagnosis of AD and similar dementias using a deep learning model. Promising results were obtained specifically with a 3D convolutional neural network trained and evaluated on the recently released OASIS-3 dataset, providing new evidence that amyloid PET can be considered a potential biomarker of neurodegeneration.

The work presented in this paper has a major limitation, relating to the way the fourth, time dimension of PET scans has been treated: the current pipeline computes the average value over time for each voxel, thus creating an "averaged" volume that is fed as input to the neural model. Although this approach has produced promising results, in order to not incur a loss of information it may be better to treat each individual scan as a time series of images. Furthermore, the proposed method could be extended in a multi-modal way, using not only amyloid PET scans, but also glucose PET scans or MRI scans. Such an extension would allow for the creation of a comprehensive diagnostic tool that may be able to detect dementia more effectively.

Acknowledgments

Data were provided by OASIS-3. Principal Investigators: T. Benzinger, D. Marcus, J. Morris; NIH P50 AG00561, P30 NS09857781, P01 AG026276, P01 AG003991, R01 AG043434, UL1 TR000448, R01 EB009352. AV-45 doses were provided by Avid Radiopharmaceuticals, a wholly owned subsidiary of Eli Lilly.

References

[1] C. Berr, J. Wancata, and K. Ritchie, "Prevalence of dementia in the elderly in Europe," *European Neuropsychopharmacology*, vol. 15, no. 4, pp. 463–471, aug 2005.

[2] K. Maiese, "Cognitive impairment and dementia: Gaining insight through circadian clock gene pathways," *Biomolecules*, vol. 11, no. 7, p. 1002, jul 2021.

[3] F. Barkhof and M. A. van Buchem, "Neuroimaging in Dementia," in *Diseases of the Brain, Head and Neck, Spine 2016-2019*, J. Hodler, R. A. Kubik-Huch, and G. K. von Schulthess, Eds. Cham: Springer International Publishing, 2016, pp. 79–85. [Online]. Available: http://link.springer.com/10.1007/978-3-319-30081-8_10

[4] D. S. Knopman, R. C. Petersen, R. H. Cha, S. D. Edland, and W. A. Rocca, "Incidence and causes of nondegenerative nonvascular dementia," *Archives of Neurology*, vol. 63, no. 2, p. 218, feb 2006.

[5] A. Fiske, M. Gatz, B. Aadnøy, and N. L. Pedersen, "Assessing age of dementia onset," *Alzheimer Disease & Associated Disorders*, vol. 19, no. 3, pp. 128–134, jul 2005.

[6] C. M. Speechly, C. Bridges-Webb, and E. Passmore, "The pathway to dementia diagnosis," *Medical Journal of Australia*, vol. 189, no. 9, pp. 487–489, nov 2008.

[7] G. Chételat, J. Arbizu, H. Barthel, V. Garibotto, I. Law, S. Morbelli, E. van de Giessen, F. Agosta, F. Barkhof, D. J. Brooks, M. C. Carrillo, B. Dubois, A. M. Fjell, G. B. Frisoni, O. Hansson, K. Herholz, B. F. Hutton, C. R. Jack, A. A. Lammertsma, S. M. Landau, S. Minoshima, F. Nobili, A. Nordberg, R. Ossenkoppele, W. J. G. Oyen, D. Perani, G. D. Rabinovici, P. Scheltens, V. L. Villemagne, H. Zetterberg, and A. Drzezga, "Amyloid-PET and 18f-FDG-PET in the diagnostic investigation of Alzheimer's disease and other dementias," *The Lancet Neurology*, vol. 19, no. 11, pp. 951–962, nov 2020.

[8] F. Altay, G. R. Sanchez, Y. James, S. V. Faraone, S. Velipasalar, and A. Salekin, "Preclinical stage Alzheimer's disease detection using magnetic resonance image scans," Nov. 2020.

[9] H. Allioui, M. Sadgal, and A. Elfazziki, "Deep MRI segmentation: A convolutional method applied to alzheimer disease detection," *International Journal of Advanced Computer Science and Applications*, vol. 10, no. 11, 2019.

[10] D. Jha and G.-R. Kwon, "Alzheimer disease detection in MRI using curvelet transform with k-NN," *Journal of Korean Institute of Information Technology*, vol. 14, no. 8, p. 121, aug 2016.

[11] A. El-Zaart and A. A.Ghosn, "MRI images thresholding for alzheimer detection," in *Computer Science & Information Technology (CS & IT)*. Academy & Industry Research Collaboration Center (AIRCC), may 2013.

[12] H. Fuse, K. Oishi, N. Maikusa, T. Fukami, and J. A. D. N. Initiative, "Detection of alzheimer's disease with shape analysis of MRI images," in *2018 Joint 10th International Conference on Soft Computing and Intelligent Systems (SCIS) and 19th International Symposium on Advanced Intelligent Systems (ISIS)*. IEEE, dec 2018.

[13] O. Ben Ahmed, J. Benois-Pineau, C. B. Amar, M. Allard, and G. Catheline, "Early alzheimer disease detection with bag-of-visual-words and hybrid fusion on structural MRI," in *2013 11th International Workshop on Content-Based Multimedia Indexing (CBMI)*. IEEE, jun 2013.

[14] L. Rice and S. Bisdas, "The diagnostic value of FDG and amyloid PET in alzheimer's disease—a systematic review," *European Journal of Radiology*, vol. 94, pp. 16–24, sep 2017.

[15] W. E. Klunk, H. Engler, A. Nordberg, Y. Wang, G. Blomqvist, D. P. Holt, M. Bergström, I. Savitcheva, G.-F. Huang, S. Estrada, B. Ausén, M. L. Debnath, J. Barletta, J. C. Price, J. Sandell, B. J. Lopresti, A. Wall, P. Koivisto, G. Antoni, C. A. Mathis, and B. Långström, "Imaging brain amyloid in Alzheimer's disease with Pittsburgh Compound-B," *Annals of Neurology*, vol. 55, no. 3, pp. 306–319, jan 2004.

[16] V. Camus, P. Payoux, L. Barré, B. Desgranges, T. Voisin, C. Tauber, R. L. Joie, M. Tafani, C. Hommet, G. Chételat, K. Mondon, V. de La Sayette, J. P. Cottier, E. Beaufils, M. J. Ribeiro, V. Gissot, E. Vierron, J. Vercouillie, B. Vellas, F. Eustache, and D. Guilloteau, "Using PET with 18f-AV-45 (florbetapir) to quantify brain amyloid load in a clinical environment," *European Journal of Nuclear Medicine and Molecular Imaging*, vol. 39, no. 4, pp. 621–631, jan 2012.

[17] A. Newberg, A. Alavi, and M. Reivich, "Determination of regional cerebral function with FDG-PET imaging in neuropsychiatric disorders," *Seminars in Nuclear Medicine*, vol. 32, no. 1, pp. 13–34, jan 2002.

TABLE I: Comparison between this work and other recent works based on deep learning. Only the best results are reported.

Reference	Dataset	Scan Type	Method	Findings
Choi et al., 2018 [19]	ADNI	FDG and AV45-PET	3D CNN, using both types of scans	AUC = 98%
Liu et al., 2018 [40]	ADNI	FDG-PET	Combination of 2D CNN and BiGRU	AUC = 95%
Ding et al., 2019 [29]	ADNI	FDG-PET	2D CNN (InceptionV3) on single slices	AUC = 98%
Altay et al., 2020 [8]	OASIS	MRI	Transformer	acc. = 91%
This work	OASIS	PiB and AV45-PET	3D CNN on averaged volumes	AUC = 87%

[18] G. D. Rabinovici, H. J. Rosen, A. Alkalay, J. Kornak, A. J. Furst, N. Agarwal, E. C. Mormino, J. P. O'Neil, M. Janabi, A. Karydas, M. E. Growdon, J. Y. Jang, E. J. Huang, S. J. DeArmond, J. Q. Trojanowski, L. T. Grinberg, M. L. Gorno-Tempini, W. W. Seeley, B. L. Miller, and W. J. Jagust, "Amyloid vs FDG-PET in the differential diagnosis of AD and FTLD," *Neurology*, vol. 77, no. 23, pp. 2034–2042, nov 2011.

[19] H. Choi and K. H. Jin, "Predicting cognitive decline with deep learning of brain metabolism and amyloid imaging," *Behavioural Brain Research*, vol. 344, pp. 103–109, may 2018.

[20] P. J. LaMontagne, T. L. S. Benzinger, J. C. Morris, S. Keefe, R. Hornbeck, C. Xiong, E. Grant, J. Hassenstab, K. Moulder, A. G. Vlassenko, M. E. Raichle, C. Cruchaga, and D. Marcus, "OASIS-3: Longitudinal neuroimaging, clinical, and cognitive dataset for normal aging and alzheimer disease," dec 2019.

[21] K. Maiese, "Impacting dementia and cognitive loss with innovative strategies: mechanistic target of rapamycin, clock genes, circular noncoding ribonucleic acids, and rho/rock," *Neural Regeneration Research*, vol. 14, no. 5, p. 773, 2019.

[22] G. Casalino, G. Castellano, K. Kaczmarek-Majer, and O. Hryniewicz, "Intelligent analysis of data streams about phone calls for bipolar disorder monitoring," in *2021 IEEE International Conference on Fuzzy Systems (FUZZ-IEEE)*. IEEE, 2021, pp. 1–6.

[23] E. Lella, A. Pazienza, D. Lofù, R. Anglani, and F. Vitulano, "An ensemble learning approach based on diffusion tensor imaging measures for Alzheimer's disease classification," *Electronics*, vol. 10, no. 3, p. 249, 2021.

[24] M. B. T. Noor, N. Z. Zenia, M. S. Kaiser, S. Al Mamun, and M. Mahmud, "Application of deep learning in detecting neurological disorders from magnetic resonance images: a survey on the detection of Alzheimer's disease, Parkinson's disease and schizophrenia," *Brain informatics*, vol. 7, no. 1, pp. 1–21, 2020.

[25] P. Scarabaggio, R. Carli, G. Cavone, N. Epicoco, and M. Dotoli, "Nonpharmaceutical stochastic optimal control strategies to mitigate the COVID-19 spread," *IEEE Transactions on Automation Science and Engineering*, 2021.

[26] G. B. Frisoni, N. C. Fox, C. R. Jack, P. Scheltens, and P. M. Thompson, "The clinical use of structural MRI in alzheimer disease," *Nature Reviews Neurology*, vol. 6, no. 2, pp. 67–77, feb 2010.

[27] B. Khagi and G.-R. Kwon, "3d CNN design for the classification of alzheimer's disease using brain MRI and PET," *IEEE Access*, vol. 8, pp. 217 830–217 847, 2020.

[28] M. Hiltunen, T. van Groen, and J. Jolkkonen, "Functional roles of amyloid-β protein precursor and amyloid-β peptides: Evidence from experimental studies," *Journal of Alzheimer's Disease*, vol. 18, pp. 401–412, 2009.

[29] Y. Ding, J. H. Sohn, M. G. Kawczynski, H. Trivedi, R. Harnish, N. W. Jenkins, D. Lituiev, T. P. Copeland, M. S. Aboian, C. M. Aparici, S. C. Behr, R. R. Flavell, S.-Y. Huang, K. A. Zalocusky, L. Nardo, Y. Seo, R. A. Hawkins, M. H. Pampaloni, D. Hadley, and B. L. Franc, "A deep learning model to predict a diagnosis of alzheimer disease by using 18f-FDG PET of the brain," *Radiology*, vol. 290, no. 2, pp. 456–464, feb 2019.

[30] S. Basheer, S. Bhatia, and S. B. Sakri, "Computational modeling of dementia prediction using deep neural network: Analysis on OASIS dataset," *IEEE Access*, vol. 9, pp. 42 449–42 462, 2021.

[31] A. V. Dalca, E. Yu, P. Golland, B. Fischl, M. R. Sabuncu, and J. E. Iglesias, "Unsupervised deep learning for bayesian brain mri segmentation," Apr. 2019.

[32] Y. Huo, Z. Xu, K. Aboud, P. Parvathaneni, S. Bao, C. Bermudez, S. M. Resnick, L. E. Cutting, and B. A. Landman, "Spatially localized atlas network tiles enables 3d whole brain segmentation from limited data," Jun. 2018.

[33] Y. Huo, Z. Xu, Y. Xiong, K. Aboud, P. Parvathaneni, S. Bao, C. Bermudez, S. M. Resnick, L. E. Cutting, and B. A. Landman, "3d whole brain segmentation using spatially localized atlas network tiles," Mar. 2019.

[34] M. Rebsamen, C. Rummel, M. Reyes, R. Wiest, and R. McKinley, "Direct cortical thickness estimation using deep learning-based anatomy segmentation and cortex parcellation," *Human Brain Mapping*, vol. 41, no. 17, pp. 4804–4814, aug 2020.

[35] J. C. Morris, "Clinical dementia rating: A reliable and valid diagnostic and staging measure for dementia of the alzheimer type," *International Psychogeriatrics*, vol. 9, no. S1, pp. 173–176, dec 1997.

[36] E. Lella and G. Vessio, "Ensembling complex network 'perspectives' for mild cognitive impairment detection with artificial neural networks," *Pattern Recognition Letters*, vol. 136, pp. 168–174, 2020.

[37] H. Zunair, A. Rahman, N. Mohammed, and J. P. Cohen, "Uniformizing techniques to process CT scans with 3D CNNs for tuberculosis prediction," Jul. 2020.

[38] N. Otsu, "A threshold selection method from gray-level histograms," *IEEE Transactions on Systems, Man, and Cybernetics*, vol. 9, no. 1, pp. 62–66, jan 1979.

[39] J. Wen, E. Thibeau-Sutre, M. Diaz-Melo, J. Samper-González, A. Routier, S. Bottani, D. Dormont, S. Durrleman, N. Burgos, O. Colliot *et al.*, "Convolutional neural networks for classification of Alzheimer's disease: Overview and reproducible evaluation," *Medical image analysis*, vol. 63, p. 101694, 2020.

[40] M. Liu, D. Cheng, and W. Y. and, "Classification of alzheimer's disease by combination of convolutional and recurrent neural networks using FDG-PET images," *Frontiers in Neuroinformatics*, vol. 12, jun 2018.